NEUROLOGY AND PRECLINICAL NEUROLOGICAL STUDIES - ORIGINAL ARTICLE

Hippocampal subfield atrophy in patients with Parkinson's disease and psychosis

Abhishek Lenka[1,2] · Madhura Ingalhalikar[6] · Apurva Shah[6] · Jitender Saini[3] · Shyam Sundar Arumugham[4] ·
Shantala Hegde[5] · Lija George[2] · Venkateswara Reddy[3] · Y. C. Janardhana Reddy[4] · Ravi Yadav[2] ·
Pramod Kumar Pal[2]

Abstract

Psychosis, manifested through formed visual hallucinations or minor hallucinations, is a common non-motor symptom of Parkinson's disease (PD). The pathogenesis of psychosis in PD remains unclear; however, is possibly linked to structural and functional alterations in the hippocampus. To explore the role of hippocampus in psychosis, a detailed hippocampal subfield analysis was performed on PD patients with (PD-P) and without psychosis (PD-NP), and healthy controls (HC). An automated subfield parcellation was performed on T1 MRI images of 141 subjects (PD-P:42, PD-NP:51, and HC:48). The volumes of 12 subfields on each side were estimated and analyzed between the three groups and were corrected for multiple comparisons using false discovery rates. The volumes were also correlated to psychosis severity and specific neuropsychological tests and finally were employed to predict the psychosis severity in PD-P using a support vector regression (SVR) model. Compared to controls, PD-NP group did not demonstrate any significant differences; however, the PD-P group had significantly lower total hippocampal volume. Bilateral molecular layer, granule cell-dentate gyrus, left subiculum, and hippocampal tail and right CA3, CA4, and HATA illustrated significantly lower volumes, while bilateral hippocampal fissure demonstrated a significant widening. Compared to PD-NP, the PD-P group had higher volume of the bilateral hippocampal fissures. Finally, SVR could significantly predict the psychosis severity from all the subfield volumes. Our findings indicate a higher degeneration of specific hippocampal subfields in PD-P compared to controls and a trend of higher volume of hippocampal fissures in PD-P group than in PD-NP.

Introduction

Psychosis is one of the frequently observed non-motor symptoms (NMS) of Parkinson's disease (PD), which commonly manifests as visual hallucinations (VH) and minor

✉ Pramod Kumar Pal
pal.pramod@rediffmail.com

1 Department of Clinical Neurosciences, National Institute of Mental Health and Neurosciences (NIMHANS), Bengaluru 560029, Karnataka, India

2 Department of Neurology, National Institute of Mental Health and Neurosciences (NIMHANS), Hosur Road, Bengaluru 560029, Karnataka, India

3 Department of Neuroimaging and Interventional Radiology, National Institute of Mental Health and Neurosciences (NIMHANS), Bengaluru 560029, Karnataka, India

4 Department of Psychiatry, National Institute of Mental Health and Neurosciences (NIMHANS), Bengaluru 560029, Karnataka, India

5 Department of Clinical Psychology, National Institute of Mental Health and Neurosciences (NIMHANS), Bengaluru 560029, Karnataka, India

6 Symbiosis Institute of Technology, Symbiosis International University, Lavale, Mulshi, Pune 412115, Maharashtra, India

hallucinatory phenomena (MH) such as sense of presence and passage (Frei and Truong 2017). The lifetime prevalence of psychosis in patients with PD is more than 50% and is associated with poor quality of life and higher healthcare resource utilization (Fredericks et al. 2017). Although numerous risk factors for VH that include older age, female gender, greater disease severity, depression, autonomic dysfunction, sleep disturbances, and cognitive impairment have been identified (Lenka et al. 2017), a comprehensive understanding of the neurobiological underpinnings of VH is hitherto lacking. Neuroimaging studies (Lenka et al. 2015), until this date, have documented structural and functional alterations in regions of the brain corresponding to the dorsal and ventral visual pathways (Goldman et al. 2014), hippocampus (Yao et al. 2016), and certain cholinergic structures such as substantia innominata (Shin et al. 2012), and pedunculopontine nucleus (Janzen et al. 2012). Based on these results, several possibilities related to the mechanism of genesis of VH in PD have been proposed. These include presence of an aberrant top-to-down visual processing unit dominating over the usual down-to-top unit and neuro-transmitter imbalance especially involving acetylcholine. In addition, alterations in the hippocampal structure and function have also been speculated to play a significant role in the emergence of VH (Lenka et al. 2017).

The hippocampus has been regarded as a site of unification of spatial and non-spatial contextual information (Goodale and Milner 1992) and is crucial in encoding and retrieval of event memories (Behrendt 2010). It has been speculated that inappropriate integration of visual information by the hippocampi could induce hallucinations instead of reflecting the reality (Olypher et al. 2006). Although the underlying mechanism remains unclear, earlier studies, especially those employing electrical stimulation of the hippocampus, have triggered complex VH in patients with epilepsy (Vignal et al. 2007). In addition, there is evidence for hippocampal involvement in schizophrenic patients with hallucinations, especially in the visual mode (Amad et al. 2014). Several lines of evidence suggest that structural and/or functional abnormalities of the hippocampi could potentially play an important role in the genesis of VH in PD. For example, autopsy studies on patients with PD and VH have revealed higher accumulation of Lewy bodies in the medial temporal lobe (Gallagher et al. 2011), while the neuroimaging studies have revealed atrophy (Ibarretxe-Bilbao et al. 2008) and altered functional connectivity of the hippocampus (Yao et al. 2016). These studies have examined the hippocampus as a single structure; however, the hippocampus is a complex structure made up of various subfields that characterize different functional aspects related to memory (Mueller et al. 2011). For instance, encoding is associated with activation in input regions in the hippocampal circuit such as the dentate gyrus (DG) and CA2-3, while

recall is related to activation in output regions such as the subiculum (Eldridge et al. 2005). In fact, significant association of atrophy of subiculum with impaired recall has been demonstrated in patients with PD (Beyer et al. 2013). It is, therefore, crucial to acquire a deeper understanding of the role of hippocampus in the pathogenesis of VH, not only by exploring it as a single structure but also by gaining insights into the specific and differential changes in the volumes of various hippocampal subfields. An earlier study has demonstrated significantly lower hippocampal subfield volumes of CA2/3, CA4/DG, and subiculum in patients with VH compared to healthy controls (HC) (Pereira et al. 2013); however, the study was carried out on a smaller sample size and employed an approximate atlas from Freesurfer 5.3 (Fischl and Dale 2000), providing coarse parcellations that included only seven subfields which did not account for the hippocampal head and tail regions (Pereira et al. 2013).

This study aims to explore and underline the hippocampal subfield volume differences on a large data set of PD patients with and without VH/MH and HC through a more sophisticated atlas (Freesurfer 6.0) (Fischl and Dale 2000; Fischl 2012) that include 12 hippocampal subfields. In addition, we aim to correlate our findings to psychosis severity as well as the neuropsychological scores pertinent to hippocampal functions, and to predict the severity of psychosis from the subfield volumes using a multi-variate prediction model.

Materials and methods

Subject recruitment and clinical evaluation

This study included 51 patients with PD without psychosis (PD-NP), 42 patients with PD with VH or MH (PD-P), and 48 age, gender, and education matched healthy HC. The patients were recruited from the general Neurology outpatient clinics and Movement Disorders services of the National Institute of Mental Health and Neurosciences (NIMHANS), Bangalore, India. All the subjects were parts of a large study aimed at identifying multi-modal biomarkers for psychosis in PD (over a period of 3.5 years: 2014 Nov–2018 April). Informed consent was obtained from all participants and the Institute Ethics Committee of NIMHANS, Bangalore, approved the study. Diagnosis of PD was based as per the UK Parkinson's disease society brain bank criteria (Hughes et al. 1992). The disease severity was evaluated using the motor section of Unified Parkinson's Disease Rating Scale (UPDRS-III) and stage of the disease was assessed as per the modified Hoehn and Yahr (H & Y) staging system. All patients underwent semi-structured interviews (by authors: AL and SSA) to explore the presence of psychiatric symptoms and the diagnosis of PD-P was based on the National Institutes of Neurological

Disorders and Stroke and National Institute of Mental Health (NINDS–NIMH) criteria for diagnosis of PD associated psychosis (Ravina et al. 2007). Severity of the psychosis was assessed using the scale proposed by Ondo et al. (2015). Details of the anti-parkinsonian medications were obtained from all the patients and total levodopa equivalent dose per day (LEDD) was calculated (Tomlinson et al. 2010). Anxiety and depression were assessed by the corresponding Hamilton rating scales (i.e. HAM-A and HAM-D). The exclusion criteria for HC included history of any neurological or psychiatric disorders or brain injuries, and family history of any neuropsychiatric disorders.

Cognitive evaluation

Cognitive functions across various domains were briefly evaluated using the Montreal Cognitive Assessment Scale (MoCA). In addition, frontal assessment battery (FAB) was used to assess the frontal executive functions (Dubois et al. 2000). As this study aimed to explore the association of the hippocampal subfield volumes with the presence of psychosis in PD, we used neuropsychological tests to assess the functions (learning and memory, visuo-spatial abilities, attention, and executive function) that are relevant to hippocampal functioning (Godsil et al. 2013; Wicking et al. 2014). Rey auditory verbal learning test (RAVLT) (Vakil and Blachstein 1993) was used to assess verbal learning and memory, complex figure test (CFT) (Shin et al. 2006) and Corsi's block-tapping test (Berch et al. 1998) were used to assess the visuo-spatial functions, and digit span was used to assess the attention of the recruited subjects. Trail making test (TMT-B) was used to assess the executive functions (Chan et al. 2008).

Image analysis

Image acquisition

Imaging data were acquired at NIMHANS, Bangalore using a Philips Achieva® 3T MRI scanner with a 32 channel head coil. High-resolution 3D T1 TFE images were acquired with repetition time (TR) = 8.1 ms, echo time (TE) = 3.7 ms, flip angle = 8°, sense factor = 3.5, field of view (FOV) = 256 × 256 × 155 mm, voxel size = 1 × 1 × 1 mm, slice thickness = 1 mm, acquisition matrix = 256 × 256, and 165 sagittal slices.

Image processing

The image-processing pipeline from Free Surfer 6.0 was adopted to pre-process the images as well as to automatically segment the hippocampal subfields (Fischl 2012). The pre-processing steps involved bias correction, automated

transformation to the Talairach reference space, intensity normalization, and removal of non-brain tissue. This was followed by segmentation of the subcortical white matter and deep gray matter nuclei, tessellation of the gray matter and white matter boundary, automated topology correction, and surface deformation to optimally place the gray/white and gray/cerebrospinal fluid boundaries. Subsequently, automated hippocampal subfield segmentation was carried out using a Bayesian inference technique that employed a probabilistic atlas of the hippocampal formation that was trained on a hybrid data set involving in-vivo ultra-high-resolution (0.1 mm) MRI and ex-vivo autopsied brain MRI from multiple subjects. Each hippocampus (left and right) was segmented into 12 subfields: CA1, CA2–3, CA4, granule cell layer of dentate gyrus (GC-DG), parasubiculum, presubiculum, subiculum, hippocampus–amygdala transition area (HATA), fimbria, molecular layer (ML-HP), hippocampal fissure (HF), and the hippocampal tail (HT). The entire hippocampus volume was considered as region 13. The description of each of these regions is provided elsewhere (Iglesias et al. 2015). Figure 1 demonstrates the automated segmentation with labeled regions in one of our subjects. Following the automated subfield extraction, volumes of each of the subfield were computed and statistical analysis was performed between the three groups. To account for different brain sizes, we normalized the subfield volumes of each subject by the total brain volume of that subject.

Statistical analysis

The analysis of demographic variables (Table 1) was performed using a standard analysis of variance test (ANOVA). For the volumetric analysis, between PD-P, PD-NP, and HC, we employed multi-variate analysis of covariance (MANCOVA) model, where the test was performed between the means of two groups under study, while age and gender were used as co-variates. Group analysis was carried out between HC vs. all patients (PD-P + PD-NP), HC vs. PD-NP, HC vs. PD-P, and PD-NP vs. PD-P. While comparing PD-P and PD-NP groups in addition to age and gender, LEDD, HAM-A, and duration of disease were also used as co-variates. Multiple comparisons were accounted for by employing False Discovery Rates (FDR) with a significance level of 0.1. The probability density functions (PDF) for each of the subfield volumes were also computed and plotted for each of the groups. Performance on the cognitive assessment was correlated with various subfield volumes separately for HC, PD-NP, and PD-P groups. The scores were initially adjusted for age and gender by means of linear regressions and the resulting standard residuals were utilized in the correlations. Pearson's r was computed and the significance of the correlation was maintained at p value < 0.01.

Fig. 1 Hippocampal subfield
segmentation on a T1 MRI
image using FreeSurfer 6.0 on
one of the HCs

Fig. 1 Hippocampal subfield segmentation on a T1 MRI image using FreeSurfer 6.0 on one of the HCs
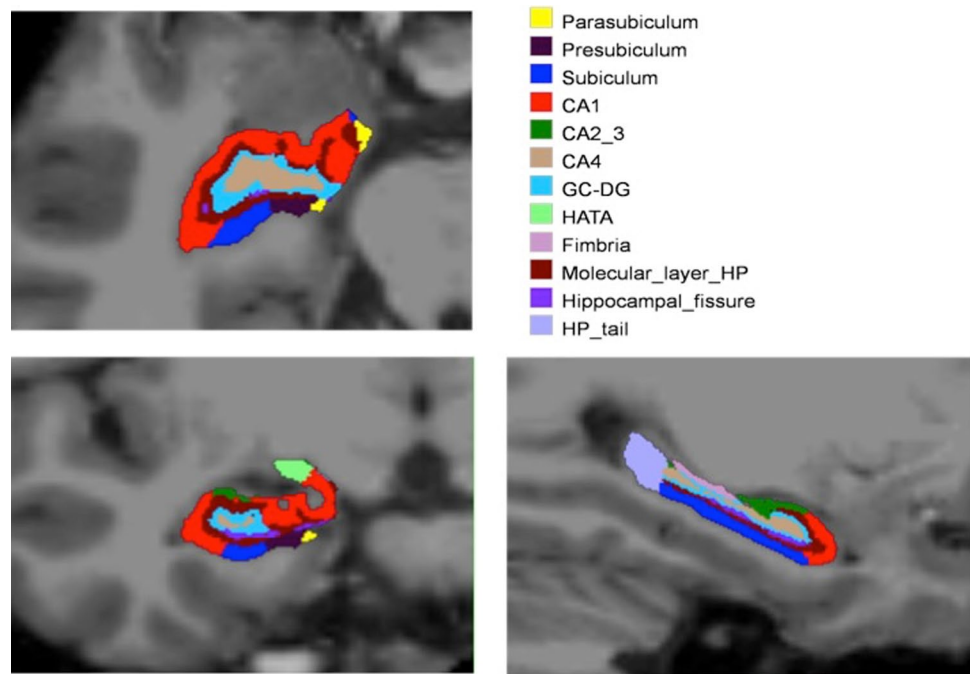
Prediction of severity in psychosis

A multi-variate model known as support vector regression (ε-SVR) algorithm (Smola and Schölkopf 2004) was employed to predict the psychosis severity scores from the hippocampal subfield volumes. SVR is a supervised learning technique based on the concept of support vector machines (SVM), but generalizes the categorical classification of SVM to predict continuous variables, which in our case was psychosis severity. SVMs model the data by finding the best separating hyperplane between data samples from two different classes by maximizing the margin between these two classes and are specified by data samples on the margin boundary known as support vectors. Similarly, in SVR, which is a regression model, the margin defined by threshold ε is minimized to achieve a superior fit to the data (Smola and Schölkopf 2004). In our case, we employed volumes of all the subfields (26) as features and severity as the predictor variable in the SVR model. A tenfold cross validation was performed, where the data were divided into ten parts, nine out of which were employed in training the SVR and the fifth one was used for testing. This process was repeated for all the folds such that every data sample was tested. Finally, the predicted scores were plotted against the severity scores and a correlation was obtained and tested for significance.

Results

Demographics, clinical characteristics, and cognitive evaluations

The three groups were matched for age and gender. The PD groups were not significantly different in terms of age at onset of PD and the duration of PD. Of those 42 patients with PD-P, 11 had isolated VH, 27 had isolated MH, and 4 had both VH and MH. Severity of motor symptoms (assessed by UPDRS-III) and stage of PD (assessed by H&Y scale) were similar in two PD groups. Both the PD groups had significantly higher HAM-A and HAM-D score compared to HC. Comparison between PD-NP and PD-P revealed higher HAM-A scores in PD-P, whereas the two groups did not have a significantly different HAM-D score. LEDD was significantly higher in the PD-P group compared to the PD-NP group (Table 1).

The overall cognitive performance as measured by MoCA revealed no difference between the PD groups, whereas the HC had significantly higher MoCA scores compared to both PD-P and PD-NP groups. FAB score, which represents frontal executive functions, were significantly low in both PD groups compared to HC, whereas the PD-P group compared to PD-NP had a lower FAB

Table 1 Demographic and clinical characteristics of the subjects

Parameters	HC ($n=48$)	PD-NP ($n=51$)	PD-P ($n=42$)	Significance
Gender (women:men)	13:35	8:43	6:36	NS
Mean age	55.4±5.1 years	57.8±6.9 years	58.7±7.7 years	NS
Age at onset of PD	–	50.9±9.8 years	52.1±7.1 years	NS
Duration of PD	–	5.8±2.4	6.6±3.2 years	NS
UPDRS-III (OFF)	–	34.6±8.2	35.2±8.4	NS
UPDRS-III (ON)	–	12.1±5.8	12.4±5.7	NS
H&Y stage	–	2.3±0.3	2.4±0.2	NS
*Total LED/day	–	565.4±203.6	729.1±318.8	$p<0.004$
Use of DA (%)		54.9%	69.0%	NS
Pramipexole (mg/day)		3.1±1.1	3.6±1.1	NS
Ropinirole (mg/day)		6.8±2.7	7.2±2.7	NS
*HAM-A	1.4±0.8	12.6±5.3	8.8±5.3	$p<0.001$ (PD-P>HC, PD-NP>HC) $p=0.008$ (PD-P>PD-NP)
HAM-D	1.3±1.9	6.9±4.8	8.6±5.5	$p<0.001$ (PD-P>HC, PD-NP>HC)
MoCA	27.9±1.4	25.4±2.6	25.8±2.7	$p<0.001$ (HC>PD-P, HC>PD-NP)
*FAB	17.0±1.0	15.5±1.6	14.5±2.1	$p<0.001$ (HC>PD-P and PD-NP) $p=0.01$ (PD-NP>PD-P)
Corsi block tapping				
Forward	5.1±0.8	4.7±0.7	4.3±0.2	$p<0.001$ (HC>PD-P)
Backward	4.3±0.7	3.9±0.6	3.6±0.6	$p<0.001$ (HC>PD-P)
*Complex figure test				
Copy	34.6±1.3	33.7±2.0	30.9±5.6	$p<0.001$ (HC>PD-P, PD-NP>PD-P)
Immediate recall	27.9±4.1	24.6±5.6	20.6±6.0	$p<0.001$ (HC>PD-P), $p=0.001$ (PD-NP>PD-P) $p=0.008$ (HC>PD-NP)
Delayed recall	24.3±4.4	21.3±5.6	17.1±5.5	$p<0.001$ (HC>PD-P), $p=0.001$ (PD-NP>PD-P) $p=0.01$ (HC>PD-NP)
Digit span				
Forward	5.4±1.1	5.1±0.9	4.7±1.0	$p=0.006$ (HC>PD-P)
Backward	4.2±0.7	3.9±0.7	3.7±0.7	$p=0.004$ (HC>PD-P)
*RAVLT				
Total learning	51.4±8.7	49.3±10.5	44.1±9.0	$p=0.001$ (HC>PD-P), $p=0.02$ (PD-NP>PD-P)
Immediate recall	11.3±1.9	10.9±2.3	9.7±2.3	$p=0.002$ (HC>PD-P), $p=0.03$ (PD-NP>PD-P)
Delayed recall	9.8±2.2	8.5±2.6	7.1±2.0	$p<0.001$ (HC>PD-P), $p=0.01$ (HC>PD-NP) $p=0.01$ (PD-NP>PD-P)
*Trail making test-B	155.6±29.7	176.6±51.2	213.0±53.7	$p<0.001$ (HC<PD-P), $p=0.001$ (PD-NP<PD-P)

HC healthy controls, *PD* Parkinson's disease, *PD-P* PD patients with psychosis, *PD-NP* PD patients without psychosis, *UPDRS-III* motor section of the Unified Parkinson's Disease Rating Scale, *H & Y* Hoehn and Yahr stage, *LED* levodopa equivalent dose, *DA* dopamine agonists (pramipexole/ropinirole), *HAM-A* Hamilton rating scale for anxiety, *HAM-D* Hamilton rating scale for depression, *MoCA* Montreal Cognitive Assessment Scale, *FAB* frontal assessment battery, *RAVLT* Rey's auditory verbal learning test

*The parameters that are significantly different between PD-NP and PD-P

score. The only difference observed in the Corsi block-tapping test and digit span test (forward and backward) was between HC and PD-P (better performance in HC). CFT revealed significantly poor performance in PD-P compared to both PD-NP and HC. In RAVLT (total learning, immediate recall, and delayed recall), PD-P performed poorly than both PD-NP and HC. In TMT-B, PD-P group performed poorly compared to both HC and PD-NP (Table 1).

Subfield volumetric analysis

From the statistical analysis on each of the normalized complete hippocampal volume, it was revealed that HC have significantly higher hippocampal volumes than the PD-P subgroup; however, there was no difference between HC and PD-NP subgroup as well as the complete PD cohort. Nonetheless, a trend of lower subfield volumes

Table 2 Volumes of all the hippocampal subfields (normalized for whole brain volume) of the three groups

Hippocampal subfields	Controls (Mean ± SD) in mm³	PD-P (Mean ± SD) in mm³	PD-NP (Mean ± SD) in mm³	HC vs. PD-P	HC vs. PD-NP	PD-P vs. PD-NP	HC vs. PD
Left HT	4.03E−04 ± 4.48E−05	3.66E−04 ± 5.50E−05	3.74E−04 ± 5.08E−05	0.012**	0.038*	0.505	0.1761
Left HF	1.08E−04 ± 2.02E−05	1.23E−04 ± 2.41E−05	1.11E−04 ± 5.70E−05	0.0116**	0.3389	0.0112*	0.0618
Left subiculum	3.07E−04 ± 3.59E−05	2.88E−04 ± 2.51E−05	2.99E−04 ± 5.96E−05	0.0458**	0.7273	0.1262	0.2559
Left presubiculum	2.18E−04 ± 2.43E−05	2.04E−04 ± 2.46E−05	2.06E−04 ± 5.71E−05	0.0703	0.1131	0.7048	0.0566
Left parasubiculum	4.10E−05 ± 6.82E−06	4.06E−05 ± 6.29E−06	4.10E−05 ± 5.93E−06	0.8146	0.9988	0.7144	0.8877
Left CA1	4.31E−04 ± 4.21E−05	4.14E−04 ± 3.86E−05	4.25E−04 ± 5.84E−05	0.1842	0.8804	0.2462	0.5989
Left CA3	1.41E−04 ± 1.32E−05	1.36E−04 ± 1.74E−05	1.39E−04 ± 5.77E−05	0.2013	0.8886	0.4232	0.6381
Left CA4	1.76E−04 ± 1.78E−05	1.67E−04 ± 1.61E−05	1.73E−04 ± 5.93E−05	0.0597	0.9674	0.1232	0.3505
Left molecular layer	3.93E−04 ± 3.76E−05	3.68E−04 ± 3.18E−05	3.82E−04 ± 5.52E−05	0.0202**	0.7066	0.2030	0.1843
Left GC-ML-DG	2.03E−04 ± 2.31E−05	1.91E−04 ± 2.02E−05	1.99E−04 ± 5.28E−05	0.0458**	0.8482	0.0825	0.2531
Left fimbria	5.12E−05 ± 1.72E−05	4.73E−05 ± 1.45E−05	4.97E−05 ± 5.12E−05	0.7785	0.9244	0.5194	0.8011
Left HATA	4.22E−05 ± 6.44E−06	4.03E−05 ± 5.87E−06	3.97E−05 ± 5.65E−06	0.2318	0.1478	0.5506	0.1055
Left whole HP	2.41E−03 ± 2.19E−04	2.26E−03 ± 1.95E−04	2.33E−03 ± 5.45E−04	0.0204**	0.4257	0.1712	0.0978
Right HT	4.03E−04 ± 4.48E−05	3.85E−04 ± 5.40E−05	3.81E−04 ± 5.30E−05	0.4081	0.1088	0.6183	0.1761
Right HF	1.16E−04 ± 2.30E−05	1.28E−04 ± 2.28E−05	1.17E−04 ± 5.19E−05	0.0252**	0.8963	0.0287*	0.1958
Right subiculum	3.08E−04 ± 2.90E−05	2.97E−04 ± 3.26E−05	3.05E−04 ± 5.32E−05	0.3444	0.7112	0.2984	0.9203
Right presubiculum	2.03E−04 ± 1.98E−05	1.94E−04 ± 2.54E−05	1.99E−04 ± 5.68E−05	0.3694	0.9524	0.3306	0.7999
Right parasubiculum	3.90E−05 ± 7.34E−06	3.80E−05 ± 6.88E−06	3.98E−05 ± 5.70E−06	0.6527	0.4655	0.2269	0.7687
Right CA1	4.58E−04 ± 4.32E−05	4.35E−04 ± 4.79E−05	4.48E−04 ± 5.78E−05	0.1457	0.9608	0.2574	0.4971
Right CA3	1.58E−04 ± 1.82E−05	1.46E−04 ± 1.87E−05	1.53E−04 ± 5.96E−05	0.0112**	0.3981	0.1297	0.0537
Right CA4	1.87E−04 ± 1.63E−05	1.75E−04 ± 1.74E−05	1.83E−04 ± 5.19E−05	0.012**	0.6947	0.1008	0.1396
Right molecular layer	4.08E−04 ± 3.41E−05	3.82E−04 ± 4.01E−05	3.97E−04 ± 5.94E−05	0.0292**	0.7943	0.1358	0.2385
Right GC-ML-DG	2.16E−04 ± 2.16E−05	2.02E−04 ± 2.21E−05	2.11E−04 ± 5.65E−05	0.0267**	0.8607	0.0935	0.2067
Right fimbria	4.84E−05 ± 1.48E−05	4.38E−05 ± 1.35E−05	4.73E−05 ± 5.30E−05	0.584	0.5978	0.2626	0.9882
Right HATA	4.56E−05 ± 5.36E−06	4.17E−05 ± 6.21E−06	4.26E−05 ± 5.39E−06	0.0146**	0.0244*	0.4905	0.0081*
Right whole HP	2.48E−03 ± 1.90E−04	2.34E−03 ± 2.31E−04	2.41E−03 ± 5.68E−04	0.0481**	0.6417	0.2128	0.2261

PD-NP Parkinson's disease with no psychosis, *PD-P* Parkinson's disease with psychosis, *HT* hippocampal tail, *HF* hippocampal formation, *CA* Cornu Ammonis, *GC* granular layer, *ML* molecular layer, *DG* dentate gyrus, *HATA* hippocampus amygdala transition area

**Corrected for multiple comparisons

*Uncorrected

(uncorrected) in PD (PD-P + PD-NP) subjects was observed in left hippocampal tail and right HATA. The differences in PD-P and HC were significantly discernible in multiple regions that involved: bilateral molecular layer, GC-DG, left subiculum and hippocampal tail and right CA3, CA4, HATA (corrected *p* value < 0.05), where PD-P demonstrated significantly lower volumes than HC (Table 2). However, only in the left and right HF, the PD-P subgroup revealed higher volume than the HC (values displayed in Table 2). Furthermore, between controls and

Fig. 2 Bar charts demonstrating the results from MANCOVA between HC and PD-P (top-left), HC and PD-NP (top-right), PD-P vs. PD-NP (bottom-left) and HC vs. all PD (bottom-right). The bars represent the normalized mean volume and the error bars are the standard deviation
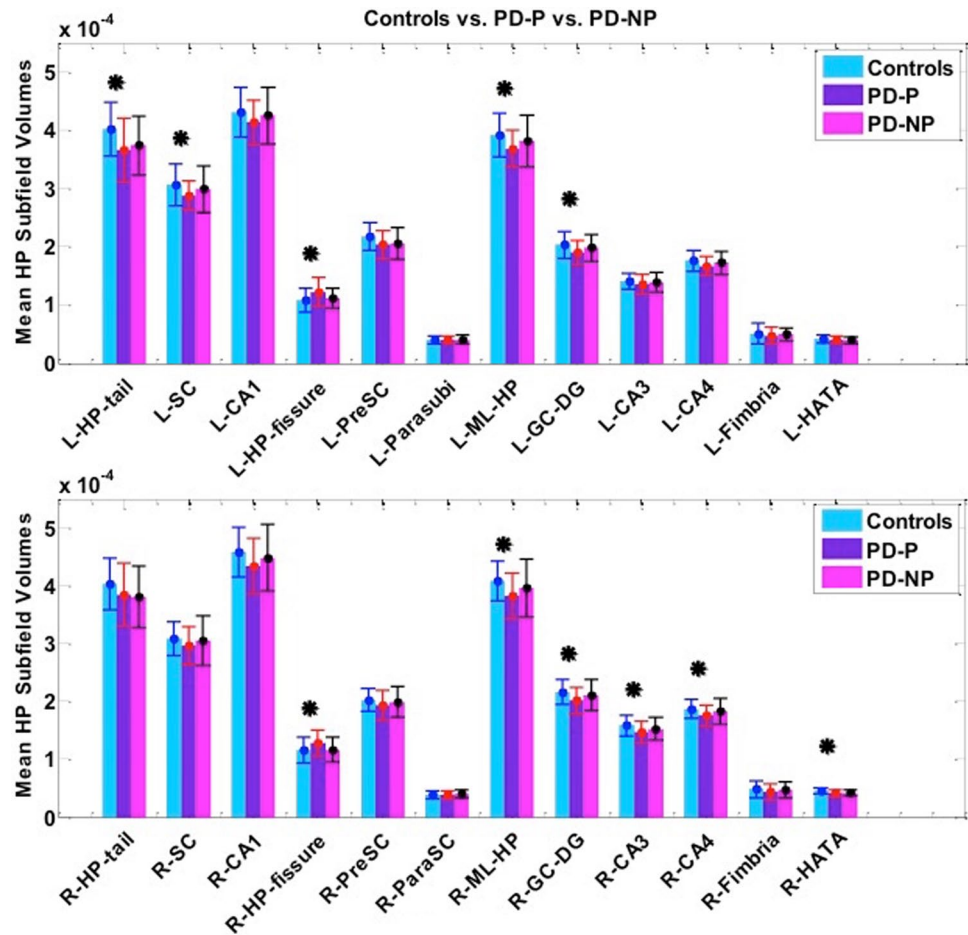
PD-NP, no significant differences were observed; however, an uncorrected trend in the left hippocampal tail and right HATA was revealed, similar to the complete PD vs. HC analysis. Finally, comparison between PD-P and PD-NP groups revealed an uncorrected significant difference in bilateral hippocampal fissure, where PD-P subgroup showed significantly higher volume than PD-NP. Bar charts in Fig. 2 and Table 2 summarize all the volumetric results.

To attain deeper understanding of the trend between PD-P and PD-NP, we plotted the PDFs of specific subfield volumes for all three groups (Fig. 3). It can be observed that the PD-P group had the lowest subfield volumes compared to the other two groups, while the PDFs of PD-NP group were either overlapped with the HC (left subiculum, left CA1, left GC-DG, and right and left hippocampal fissure) or lied in between HC and PD-P (left and right molecular layer, right CA3, right CA4, right GC-DG, R-HATA, and bilateral total hippocampal volume) (Fig. 3). Only the HF demonstrated an opposite trend, where the PD-P group illustrated highest volumes in comparison with PD-NP and HC, as shown in Fig. 3.

Correlation of the subfield volumes with parameters of cognition

Analysis for the correlation of the subfield volumes and the cognitive parameters was done for the PD groups (Table 3; Fig. 4). In the PD-P group—(1) the FAB score had a significant positive correlation ($p < 0.01$) with the volume of left fimbria and (2) the psychosis severity score had a negative correlation with the left CA3 volume. Other correlations with p value < 0.05 have been provided in Table 3 and their plots in the supplementary material (Supp. Figure 1). The key findings were the negative correlation of psychosis severity with right CA3 (p value $= 0.011$) and a negative correlation between CFT (copy) score and left hippocampal fissure volume (p value $= 0.05$).

Predicting the psychosis severity

The multi-variate SVR model demonstrated a precise prediction of psychosis severity from all the hippocampal subfield volumes together. A tenfold cross validation revealed that severity scores could be predicted accurately
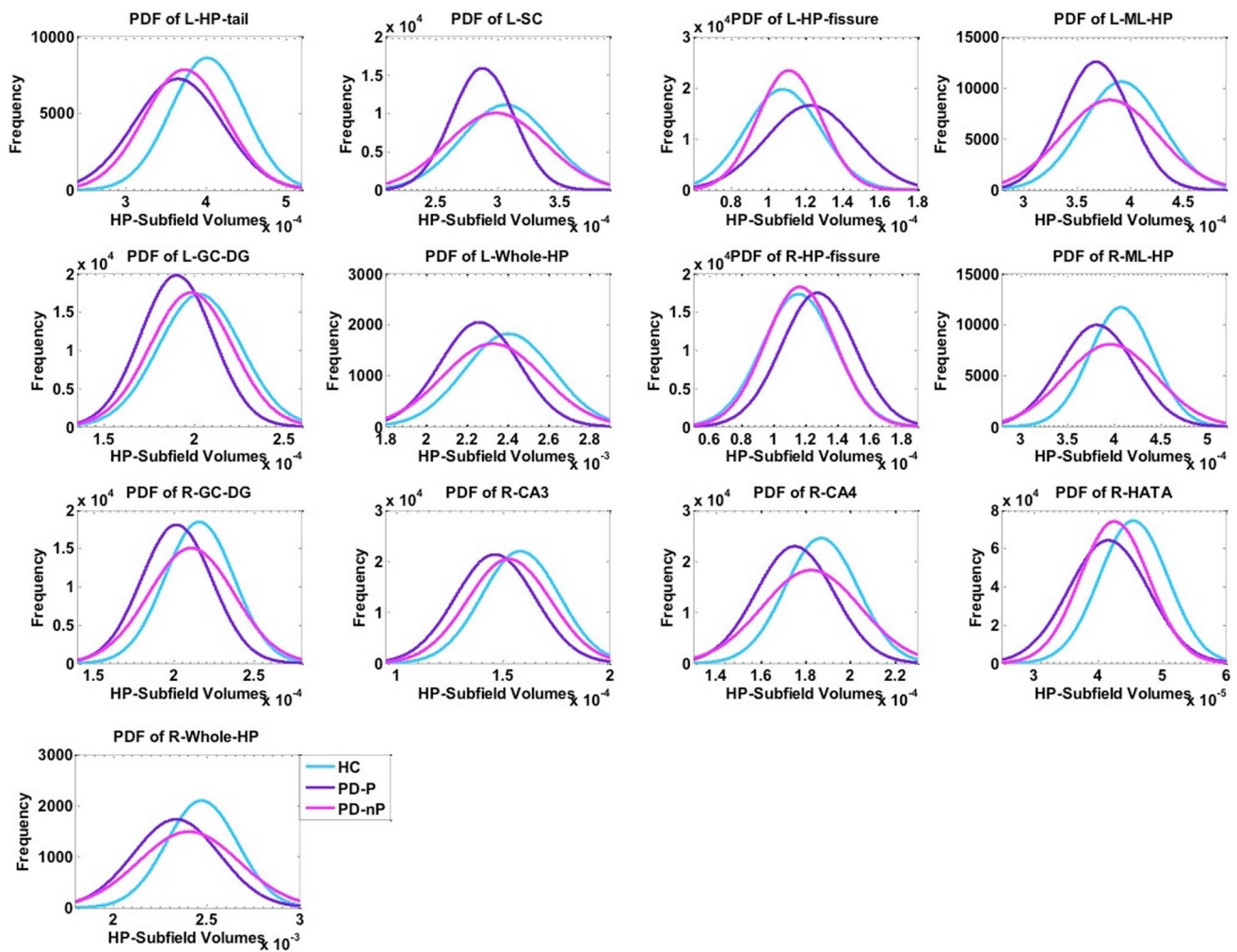
Fig. 3 Figure displays the PDFs of the subfield volumes in the three groups (HC, PD-P, and PD-NP). The PD-P (purple) has its PDF is on the leftmost side, while PD-NP (pink) lies in the middle of PD-P and HC and demonstrates high variability compared to PD-P group

Table 3 Summary of correlation analysis between volume of hippocampal subfields in PD-P group and scores of the neuropsychological examinations

Tests	Subfield	r	p value
RAVLT (delayed recall)	Left subiculum	0.32	0.03
	Left ML	0.30	0.04
	Right fimbria	0.31	0.04
FAB	Right fimbria	0.45	0.002
CFT (copy)	Right HF	−0.29	0.05
	Right fimbria	0.33	0.03
Psychosis severity	Left-CA3	−0.30	0.01
	Right CA3	−0.38	0.01
	Left parasubiculum	0.32	0.03

PD-P Parkinson's disease with psychosis, *RAVLT* Rey Auditory Verbal Learning Test, *HF* Hippocampal formation, *CA* Cornu Ammonis, *ML* molecular layer

(p value $= 0.009$, when tested for correlation), with a correlation coefficient of 0.4. Figure 5 demonstrates the plot of baseline scores vs. the predicted scores.

Discussion

In this study, we compared the volumes of the hippocampal subfields of PD-P, PD-NP, and HC and correlated these volumes to psychosis severity as well as scores of representing several cognitive domains. In addition, we employed advanced SVR model to predict the psychosis severity index. Our findings not only endorsed earlier discoveries, but also provided deeper insights into the bidirectional volumetric changes that occur with psychosis and their cognitive associations. Moreover, using multi-variate regression method, we demonstrated that the trajectory of psychosis severity could be mapped using hippocampal subfield volumes. The key

Fig. 4 Correlation of the volumes of hippocampal subfields with scores of neuropsychological tests and psychosis severity (results with $p < 0.01$)

Correlation of R-fimbria vs FAB
R = 0.458

Correlation of L-CA3 vs Severity
R = -0.395

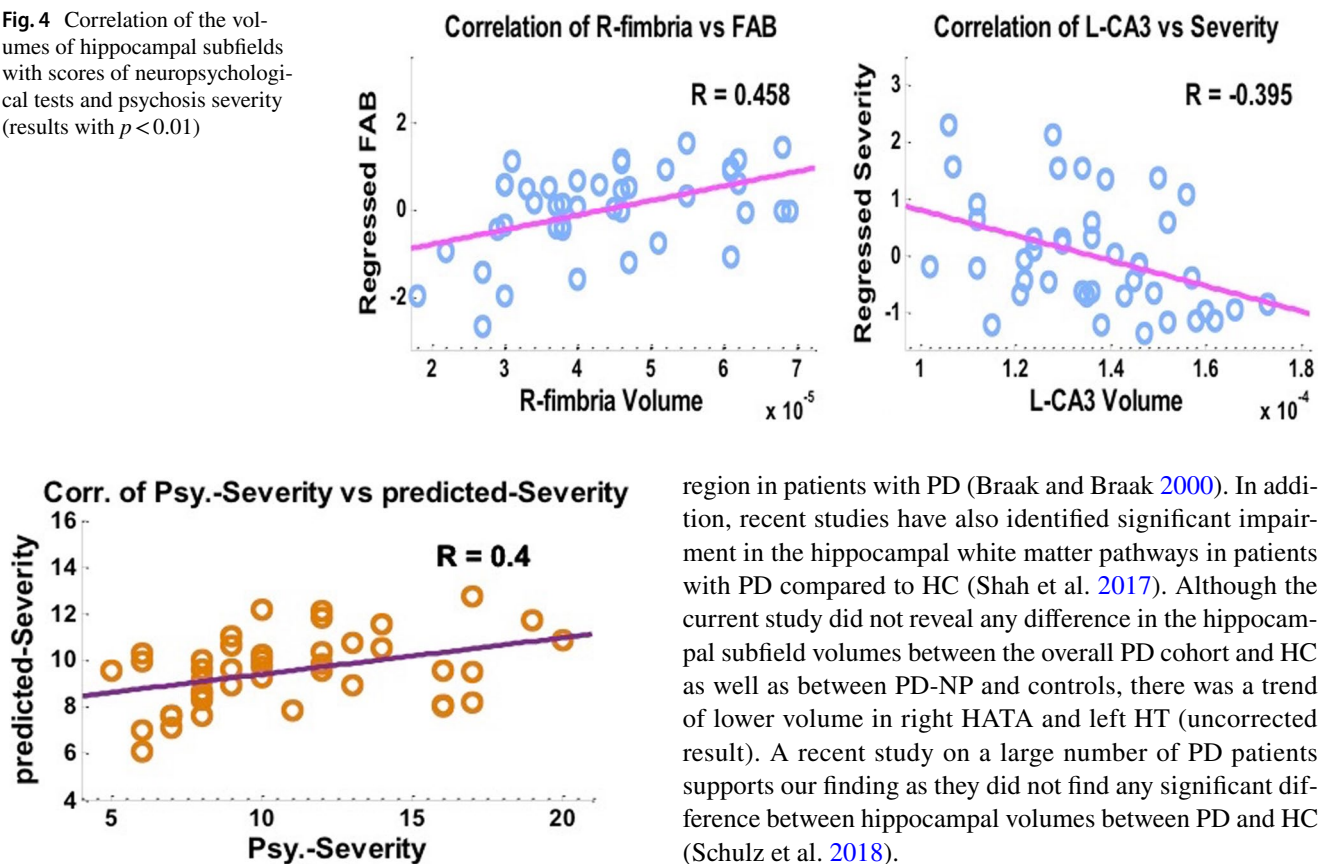

Corr. of Psy.-Severity vs predicted-Severity
R = 0.4

Fig. 5 Plot of baseline scores vs. the predicted scores obtained through support vector regression

findings of this study included: (1) total hippocampal volume as well as widespread subfield volume reduction in the PD-P group compared to HC; (2) larger hippocampal fissure volume in PD-P in comparison with controls and PD-NP; (3) significant negative association between the CA3 volumes with psychosis severity scores, as well as significant specific associations with cognitive functions; and (4) high accuracy in predicting psychosis severity in PD-P subjects from the hippocampal subfields.

Hippocampal involvement in PD has received a great deal of attention since the identification of a wide range of non-motor symptoms in PD. Growing evidence from clinical observations and experimental studies suggests a complex hippocampal cross talk among the dopaminergic and other transmitter systems which is crucial for synaptic plasticity, adaptive memory, and motivated behavior (Calabresi et al. 2013). Earlier studies have documented degeneration of hippocampal subfield CA2-3 in autopsy studies on demented as well as non-demented patients with PD (Mattila et al. 1999; Harding and Halliday 2001) as well as via MRI-based analyses (Beyer et al. 2013; Pereira et al. 2013). Moreover, the presence of Lewy neurites has been documented in the CA-2

region in patients with PD (Braak and Braak 2000). In addition, recent studies have also identified significant impairment in the hippocampal white matter pathways in patients with PD compared to HC (Shah et al. 2017). Although the current study did not reveal any difference in the hippocampal subfield volumes between the overall PD cohort and HC as well as between PD-NP and controls, there was a trend of lower volume in right HATA and left HT (uncorrected result). A recent study on a large number of PD patients supports our finding as they did not find any significant difference between hippocampal volumes between PD and HC (Schulz et al. 2018).

One of the key results of this study was higher volume of the hippocampal fissure in PD-P group compared to both PD-NP and HC (uncorrected). Moreover, there was a significant negative correlation (at significance level of $p < 0.05$) between the volumes of hippocampal fissure and the score of CFT (copy), which represents visual memory and visuo-spatial functions. HF dilation, during the course of hippocampal atrophy, has been recently established from a mouse hippocampus study that demonstrated that the increase in HF volume is highly correlated with decrease in the overall hippocampal volume and can be considered as a radiological hallmark of ongoing hippocampal atrophy (Li et al. 2018). Existing studies in Alzheimer's disease and schizophrenia have also confirmed widening of the HF in patients and have related to medial temporal lobe atrophy (Smith et al. 2003; De Bastos-Leite et al. 2006). The aforementioned evidence indicates that HF hypertrophy perhaps heralds atrophy of hippocampus. Since we did not find any difference in the remaining subfields between PD-NP and PD-P, it is possible that the PD-P group in our study in the early stage of a process leading to hippocampal atrophy and longitudinal evaluations may provide more insights into the same.

The comparison between HC and PD-P revealed significant reduction in the volumes of left subiculum, granule cell-dentate gyrus, right CA3, CA4, bilateral molecular layer, hippocampal tail, and HATA in PD-P. Subiculum has been implicated in memory and recall process and the previous

studies have documented atrophy of the subiculum in PD patients with VH (Pereira et al. 2013) as well as in patients with Alzheimer's disease (Bobinski et al. 2000; Mueller et al. 2011). The possible role of subiculum in the aforementioned cognitive processed gets support from our correlation analysis, which revealed a significant positive correlation of volume of the left subiculum with scores of AVLT (delayed recall) (sup. figure-1). Our study also demonstrated the associations between the CA3 subfield volumes (Fig. 4 and Supp. Figure 1) and psychosis severity suggesting putative role of CA3 in generating hallucinations. Although the exact mechanism by which structural alterations in CA3 result in hallucinations is not clear, aberrant connections between CA3 and CA1 have been implicated in the genesis of positive symptoms in patients with schizophrenia (Tamminga et al. 2010). It is posited that these hippocampal subfields act as a binding module for the cortical circuits comprising weakly related sensory representations. Moreover, CA3 in particular has been speculated to generate representations of space and time as a basis of conscious awareness (Behrendt 2010). Hence, the resultant sensory disintegration secondary to atrophy of the aforementioned subfields is perhaps responsible for the genesis of hallucinations. Furthermore, with regard to the notion that hyper-dopaminergic state may induce psychosis (Tost et al. 2010), it has been hypothesized that disinhibition of hippocampal subfields may favor hyper-dopaminergic states, thus resulting into psychosis (Lisman et al. 2008).

In addition, animal studies have reported that lesions in the fimbria and/or amygdala result in impaired visuo-spatial functions, and object discrimination and interestingly, visuo-spatial dysfunction, and poor object discrimination have been reported in PD patients with hallucinations (Lenka et al. 2016a). Our results corroborate this by revealing a positive correlation between right fimbria volume and FAB scores (Fig. 4) and with CFT (copy) (Supp. Figure 1). The PD-P group also illustrated atrophy of the subfield representing the GC-DG, which is an important input region of the hippocampus. Several lines of evidence indicate that the DG participates in the pre-processing of incoming information, preparing it for subsequent processing in CA3 (Jonas and Lisman 2014). Moreover, the DG is probably involved in pattern separation, transforming relatively similar input patterns into substantially different output patterns. Hence, it is possible that structural and functional alterations in the DG may precipitate hallucinations.

We observed a distinct trend between the groups via the PDF plots (Fig. 3), where the HC demonstrated highest subfield volumes, whereas the PD-NP either overlapped with HC or were located in between HCs and PD-Ps. This trend was observed only in specific subfields, as shown in Fig. 3. This trend indicates that genesis of minor or visual hallucination perhaps parallels to that of progressive

hippocampal atrophy. Overall, our analysis provides novel insights into the role of hippocampus in PD-P. The core volumetric changes occurring in the hippocampus could provide a direct indication of the severity of psychosis, as shown in Fig. 5. The multi-variate model could capture the bidirectional volumetric alterations that spanned over all the hippocampal subfields to predict the severity of hallucinations. Such a model can be further tested and employed to quantify the pathology through structural changes.

In this study, we had a relatively limited but focused scope to investigate the alterations in hippocampal subfields in PD-P. The interpretation is largely limited to hippocampal function, which is one of the limitations of this study. Cross-sectional design of the study was another limitation as patients who did not have psychosis at the time of the study may develop psychosis in future. It may also be argued that the volume changes in the hippocampal subfields, which we have noticed in PD-P group compared to HC, are more representative of the cognitive dysfunction in the PD-P rather than the psychosis. However, it is known that psychosis and cognitive dysfunction usually coexist as part of PD non-motor symptoms and it is possible that both these symptoms have overlapping neural correlates (Lenka et al. 2016b). As cross-sectional studies provide limited inference regarding the exact association between them, future studies involving longitudinal design may aid in achieving deeper insights.

Conclusion

In summary, we conclude that patients with PD-P have atrophy of several hippocampal subfields compared to HC. The volumetric changes in PD-P are differential in nature, as majority of the subfields had lower volume (compared to controls), whereas the HF had increased volume (compared to both HC and PD-NP) and the volume changes had significant correlations with specific cognitive functions. In addition, the CA3 subfield volumes in PD-P illustrated a strong correlation with severity of psychosis, thus facilitating deeper understanding of the role of hippocampus in VHs. The study reinforces the possibility that structural alterations in specific hippocampal regions in PD-P are associated with cognitive impairment and hippocampal subfield volumetry merits further exploration in this context.

Compliance with ethical standards

Conflict of interest None of the authors have any financial disclosure to make or have any conflict of interest.

References

Amad A, Cachia A, Gorwood P et al (2014) The multimodal connectivity of the hippocampal complex in auditory and visual hallucinations. Mol Psychiatry 19:184–191. https://doi.org/10.1038/mp.2012.181

Behrendt RP (2010) Contribution of hippocampal region CA3 to consciousness and schizophrenic hallucinations. Neurosci Biobehav Rev 34:1121–1136

Berch DB, Krikorian R, Huha EM (1998) The Corsi block-tapping task: methodological and theoretical considerations. Brain Cogn 38(3):317–338. https://doi.org/10.1006/brcg.1998.1039

Beyer MK, Bronnick KS, Hwang KS et al (2013) Verbal memory is associated with structural hippocampal changes in newly diagnosed Parkinson's disease. J Neurol Neurosurg Psychiatry 84:23–28. https://doi.org/10.1136/jnnp-2012-303054

Bobinski M, de Leon MJ, Wegiel J et al (2000) The histological validation of post mortem magnetic resonance imaging-determined hippocampal volume in Alzheimer's disease. Neuroscience 95:721–725. https://doi.org/10.1016/S0306-4522(99)00476-5

Braak H, Braak E (2000) Pathoanatomy of Parkinson's disease. J Neurol 247(Suppl):II3–I10. https://doi.org/10.1007/PL00007758

Calabresi P, Castrioto A, Di Filippo M, Picconi B (2013) New experimental and clinical links between the hippocampus and the dopaminergic system in Parkinson's disease. Lancet Neurol 12:811–821

Chan RCK, Shum D, Toulopoulou T, Chen EYH (2008) Assessment of executive functions: review of instruments and identification of critical issues. Arch Clin Neuropsychol 23:201–216. https://doi.org/10.1016/j.acn.2007.08.010

De Bastos-Leite AJ, Van Waesberghe JH, Oen AL et al (2006) Hippocampal sulcus width and cavities: comparison between patients with Alzheimer disease and nondemented elderly subjects. Am J Neuroradiol 27:2141–2145

Dubois B, Slachevsky A, Litvan I, Pillon B (2000) The FAB: a frontal assessment battery at bedside. Neurology 55:1621–1626. https://doi.org/10.1212/WNL.57.3.565

Eldridge LL, Engel SA, Zeineh MM et al (2005) A dissociation of encoding and retrieval processes in the human hippocampus. J Neurosci 25:3280–3286. https://doi.org/10.1523/jneurosci.3420-04.2005

Fischl B (2012) FreeSurfer. Neuroimage 62:774–781

Fischl B, Dale AM (2000) Measuring the thickness of the human cerebral cortex from magnetic resonance images. Proc Natl Acad Sci 97:11050–11055. https://doi.org/10.1073/pnas.200033797

Fredericks D, Norton JC, Atchison C et al (2017) Parkinson's disease and Parkinson's disease psychosis: a perspective on the challenges, treatments, and economic burden. Am J Manag Care 23:S83–S92. https://doi.org/10.1002/mds.25292

Frei K, Truong DD (2017) Hallucinations and the spectrum of psychosis in Parkinson's disease. J Neurol Sci 374:56–62

Gallagher DA, Parkkinen L, O'Sullivan SS et al (2011) Testing an aetiological model of visual hallucinations in Parkinson's disease. Brain 134:3299–3309. https://doi.org/10.1093/brain/awr225

Godsil BP, Kiss JP, Spedding M, Jay TM (2013) The hippocampal-prefrontal pathway: the weak link in psychiatric disorders? Eur Neuropsychopharmacol 23:1165–1181

Goldman JG, Stebbins GT, Dinh V et al (2014) Visuoperceptive region atrophy independent of cognitive status in patients with Parkinson's disease with hallucinations. Brain 137:849–859. https://doi.org/10.1093/brain/awt360

Goodale MA, Milner AD (1992) Separate visual pathways for perception and action. Trends Neurosci 15:20–25

Harding AJ, Halliday GM (2001) Cortical Lewy body pathology in the diagnosis of dementia. Acta Neuropathol 102:355–363. https://doi.org/10.1007/s004010100390

Hughes AJ, Daniel SE, Kilford L, Lees AJ (1992) Accuracy of clinical diagnosis of idiopathic Parkinson's disease: a clinicopathological study of 100 cases. J Neurol Neurosurg Psychiatry 55:181–184. https://doi.org/10.1136/jnnp.55.3.181

Ibarretxe-Bilbao N, Ramírez-Ruiz B, Tolosa E et al (2008) Hippocampal head atrophy predominance in Parkinson's disease with hallucinations and with dementia. J Neurol 255:1324–1331. https://doi.org/10.1007/s00415-008-0885-8

Iglesias JE, Augustinack JC, Nguyen K et al (2015) A computational atlas of the hippocampal formation using ex vivo, ultra-high resolution MRI: application to adaptive segmentation of in vivo MRI. Neuroimage 115:117–137. https://doi.org/10.1016/j.neuroimage.2015.04.042

Janzen J, van't Ent D, Lemstra AW et al (2012) The pedunculopontine nucleus is related to visual hallucinations in Parkinson's disease: preliminary results of a voxel-based morphometry study. J Neurol 259:147–154. https://doi.org/10.1007/s00415-011-6149-z

Jonas P, Lisman J (2014) Structure, function, and plasticity of hippocampal dentate gyrus microcircuits. Front Neural Circuits 8:107

Lenka A, Jhunjhunwala KR, Saini J, Pal PK (2015) Structural and functional neuroimaging in patients with Parkinson's disease and visual hallucinations: a critical review. Parkinsonism Relat Disord 21:683–691. https://doi.org/10.1016/j.parkreldis.2015.04.005

Lenka A, Hegde S, Arumugham SS, Pal PK (2016a) Pattern of cognitive impairment in patients with Parkinson's disease and psychosis: a critical review. Parkinsonism Relat Disord 26:1814–1824. https://doi.org/10.1016/j.parkreldis.2016.12.025

Lenka A, Hegde S, Jhunjhunwala KR, Pal PK (2016b) Interactions of visual hallucinations, rapid eye movement sleep behavior disorder and cognitive impairment in Parkinson's disease: a review. Parkinsonism Relat Disord 22:1–8. https://doi.org/10.1016/j.parkreldis.2015.11.018

Lenka A, Herath P, Christopher R, Pal PK (2017) Psychosis in Parkinson's disease: from the soft signs to the hard science. J Neurol Sci 379:169–176

Li Y, Yan J, Zhu X et al (2018) Increased hippocampal fissure width is a sensitive indicator of rat hippocampal atrophy. Brain Res Bull 137:91–97. https://doi.org/10.1016/j.brainresbull.2017.11.014

Lisman JE, Coyle JT, Green RW et al (2008) Circuit-based framework for understanding neurotransmitter and risk gene interactions in schizophrenia. Trends Neurosci 31:234–242. https://doi.org/10.1016/j.tins.2008.02.005

Mattila PM, Rinne JO, Helenius H, Röyttä M (1999) Neuritic degeneration in the hippocampus and amygdala in Parkinson's disease in relation to Alzheimer pathology. Acta Neuropathol 98:157–164. https://doi.org/10.1007/s004010051064

Mueller SG, Chao LL, Berman B, Weiner MW (2011) Evidence for functional specialization of hippocampal subfields detected by MR subfield volumetry on high resolution images at 4T. Neuroimage 56:851–857. https://doi.org/10.1016/j.neuroimage.2011.03.028

Olypher AV, Klement D, Fenton AA (2006) Cognitive disorganization in hippocampus: a physiological model of the disorganization in psychosis. J Neurosci 26:158–168. https://doi.org/10.1523/JNEUROSCI.2064-05.2006

Ondo WG, Sarfaraz SAS, Lee M (2015) A novel scale to assess psychosis in patients with parkinson's disease. J Clin Mov Disord 2:17. https://doi.org/10.1186/s40734-015-0024-5

Pereira JB, Junqué C, Bartrés-Faz D et al (2013) Regional vulnerability of hippocampal subfields and memory deficits in Parkinson's disease. Hippocampus 23:720–728. https://doi.org/10.1002/hipo.22131

Ravina B, Marder K, Fernandez HH et al (2007) Diagnostic criteria for psychosis in Parkinson's disease: report of an NINDS, NIMH Work Group. Mov Disord 22:1061–1068

Schulz J, Pagano G, Fernández Bonfante JA et al (2018) Nucleus basalis of Meynert degeneration precedes and predicts cognitive impairment in Parkinson's disease. Brain 75:373–387. https://doi.org/10.1093/brain/awy072

Shah A, Lenka A, Saini J, Wagle S, Naduthota RM, Yadav R, Pal PK, Ingalhalikar M (2017) Altered brain wiring in Parkinson's disease: a structural connectome based analysis. Brain Connect. https://doi.org/10.1089/brain.2017.0506

Shin MS, Park SY, Park SR et al (2006) Clinical and empirical applications of the Rey-Osterrieth Complex Figure Test. Nat Protoc 1:892–899. https://doi.org/10.1038/nprot.2006.115

Shin S, Lee JE, Hong JY et al (2012) Neuroanatomical substrates of visual hallucinations in patients with non-demented Parkinson's disease. J Neurol Neurosurg Psychiatry 1155–1162. https://doi.org/10.1136/jnnp-2012-303391

Smith GN, Lang DJ, Kopala LC et al (2003) Developmental abnormalities of the hippocampus in first-episode schizophrenia. Biol Psychiatry 53:555–561. https://doi.org/10.1016/S0006-3223(02)01977-7

Smola AJ, Schölkopf B (2004) A tutorial on support vector regression. Stat Comput 14:199–222

Tamminga CA, Stan AD, Wagner AD (2010) The hippocampal formation in schizophrenia. Am J Psychiatry 167:1178–1193

Tomlinson CL, Stowe R, Patel S et al (2010) Systematic review of levodopa dose equivalency reporting in Parkinson's disease. Mov Disord 25:2649–2653. https://doi.org/10.1002/mds.23429

Tost H, Alam T, Meyer-Lindenberg A (2010) Dopamine and psychosis: theory, pathomechanisms and intermediate phenotypes. Neurosci Biobehav Rev 34:689–700

Vakil E, Blachstein H (1993) Rey Auditory-Verbal Learning Test: structure analysis. J Clin Psychol 49(6):883–890. https://doi.org/10.1002/1097-4679(199311)49:6%3C883::AID-JCLP2270490616%3E3.0.CO;2-6

Vignal JP, Maillard L, McGonigal A, Chauvel P (2007) The dreamy state: Hallucinations of autobiographic memory evoked by temporal lobe stimulations and seizures. Brain 130:88–99. https://doi.org/10.1093/brain/awl329

Wicking M, Nees F, Steiger F (2014) Neuropsychological measures of hippocampal function. Front Neurol Neurosci 34:60–70. https://doi.org/10.1159/000356425

Yao N, Cheung C, Pang S et al (2016) Multimodal MRI of the hippocampus in Parkinson's disease with visual hallucinations. Brain Struct Funct 221:287–300. https://doi.org/10.1007/s00429-014-0907-5